ELSEVIER

Inorganica Chimica Acta 240 (1995) 99–104

Inorganica Chimica Acta

Kinetics and mechanisms of ligand substitution reactions of molybdenum SO_2 complexes. Synthesis and X-ray structure of *trans*-$Mo(CO)_2(dmpe)(PPh_3)(SO_2)$ ☆

Jian-Kun Shen [a,*], Gregory J. Kubas [b], Arnold L. Rheingold [c,*]

[a] *Department of Chemistry, Northwestern University, Evanston, IL 60208, USA*

[b] *Material and Chemical Design Group, CST-10:MS-C346, Los Alamos National Laboratory, Los Alamos, NM 87545, USA*

[c] *Department of Chemistry, University of Delaware, Newark, DE 19716, USA*

Received 21 December 1994; revised 24 March 1995

Abstract

Kinetic results are reported for intramolecular PPh_3 substitution reactions of $Mo(CO)_2(\eta^1\text{-L})(PPh_3)_2(SO_2)$ to form $Mo(CO)_2(\eta^2\text{-L})(PPh_3)(SO_2)$ (L = dmpe = $(Me)_2PC_2H_4P(Me)_2$ and dppe = $Ph_2PC_2H_4PPh_2$) in THF solvent, and for intermolecular SO_2 substitutions in $Mo(CO)_3(\eta^2\text{-L})(\eta^2\text{-}SO_2)$ (L = 2,2′-bipyridine, dppe) with phosphorus ligands in CH_2Cl_2 solvent. Activation parameters for intramolecular PPh_3 substitution reactions: ΔH^* values are 12.3 kcal/mol for dmpe and 16.7 kcal/mol for dppe; ΔS^* values are -30.3 cal/mol K for dmpe and -16.4 cal/mol K for dppe. These results are consistent with an intramolecular associative mechanism. Substitutions of SO_2 in $Mo(CO)_3(\eta^2\text{-L})(\eta^2\text{-}SO_2)$ complexes proceed by both dissociative and associative mechanisms. The facile associative pathways for the reactions are discussed in terms of the ability of SO_2 to accept a pair of electrons from the metal, with its bonding transformation of η^2-SO_2 to η^1-pyramidal SO_2, maintaining a stable 18-e count for the complex in its reaction transition state. The structure of $Mo(CO)_2(dmpe)(PPh_3)(SO_2)$ was determined crystallographically: $P2_1/c$, $a = 9.311(1)$, $b = 16.344(2)$, $c = 18.830(2)$ Å, $\beta = 91.04(1)°$, $V = 2865.1(7)$ Å^3, $Z = 4$, $R(F) = 3.49\%$.

Keywords: Kinetics and mechanism; Ligand substitution reactions; Crystal structures; Molybdenum complexes; Sulfur dioxide complexes

1. Introduction

Basolo and co-workers first reported in 1966 that ligand substitution reactions of some 18-e complexes containing NO [1], cyclopentadienyl [2] or benzene [3] ligands proceeded by associative pathways. It was suggested [1–3] that the presence of these ligands permits the associative substitution reactions by localizing a pair of electrons on the ligand in the reaction transition state, thus maintaining a stable 18-e count throughout the reaction pathway. The localization of a pair of electrons on the ligand is allowed by ligand coordination mode changes, such as ring slippage of cyclopolyolefins from η^n to η^{n-2}. Such ligand hapticity changes which generate an open coordination site have become important fundamental components of certain organometallic reactions [4a,b].

Considerable research has been done with the ring metal compounds in terms of ring-slippage processes [4a], but far less has been done on systems containing NO-like ligands, such as SO_2. NO can be bonded to a metal in either a linear fashion M=N=O, or a pair of non-bonding electrons can be localized on the nitrogen resulting in a bent sp^2 hybrid nitrosyl [5] M–N=O. This then frees a metal orbital for attack by the entering nucleophile resulting in a low energy associative displacement reaction via a stable 18-e transition state [1].

It has long been known [6] that SO_2 is both a Lewis acid and a Lewis base. Its base behavior has metal–SO_2 bonding modes of the structural types [7] η^1-planar (see I) or η^2 (see II) where SO_2 donates a pair of electrons to the metal accompanied by π-backbonding from filled d orbitals of the metal atom. The Lewis acid behavior of SO_2 as a ligand results in an η^1-pyramidal (see III) bonding mode where SO_2 accepts a pair of electrons from the metal.

☆ Dedicated to Professor Fred Basolo on his 75th birthday.

* Corresponding authors.

SSDI 0020-1693(95)04649-T

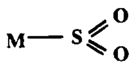

I

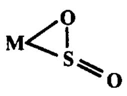

II

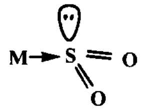

III

These bonding modes suggest the ligand SO$_2$, in a manner analogous to NO, may possibly mediate an associative displacement reaction of an 18-e monomeric organometallic compound. For example, the then presumed reaction mechanism can be illustrated in general by Eq. (1).

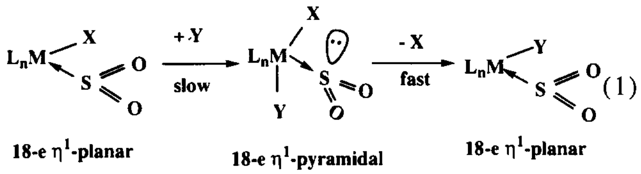

This hypothetical case shows that SO$_2$ shifts from Lewis base to Lewis acid behavior, thus allowing the entering nucleophile Y to attack the metal whilst still maintaining a stable 18-e count for the active intermediate. In spite of this seemingly plausible ligand substitution mechanism, prior to our preliminary communication [8] there seems to be no report in the literature of its having been observed.

This paper reports kinetic results on ligand substitution reactions of some molybdenum SO$_2$ complexes (Eqs. (2) and (3)).

$$\mathrm{Mo(CO)_2(\eta^1\text{-}L)(PPh_3)_2(SO_2)} \longrightarrow \mathrm{Mo(CO)_2(\eta^2\text{-}L)(PPh_3)(SO_2) + PPh_3} \quad (2)$$

L = dppe, dmpe

$$\mathrm{Mo(CO)_3(\eta^2\text{-}L)(\eta^2\text{-}SO_2) + PR_3} \longrightarrow \mathrm{Mo(CO)_3(\eta^2\text{-}L)PR_3 + SO_2} \quad (3)$$

L = bipy, dppe

The facile associative pathways observed in these reactions suggest that interconversion of SO$_2$ coordination modes plays an important role in the ligand substitution processes.

2. Experimental

2.1. Reagents

THF was distilled under N$_2$ from sodium benzophenone-ketyl. The complexes Mo(CO)$_2$(PPh$_3$)$_2$(η^2-SO$_2$)(NCMe), *fac*-Mo(CO)$_3$(bipy)(η^2-SO$_2$) and Mo(CO)$_4$(dppe) (dppe = Ph$_2$PC$_2$H$_4$PPh$_2$) were synthesized according to literature methods [9,10]. P(n-Bu)$_3$ and C$_2$H$_4$(PMe$_2$)$_2$ were distilled under N$_2$ from sodium before use. PPh$_3$ and Ph$_2$PC$_2$H$_4$PPh$_2$ were recrystallized from ethyl alcohol.

2.2. Preparation of *fac*-Mo(CO)$_3$(dppe)(η^2-SO$_2$) [9]

80 mg of Mo(CO)$_4$(dppe) were dissolved in 40 ml of THF. The solution was irradiated with a medium-pressure mercury arc lamp for 2 h under a flow of N$_2$. The pale yellow solution turned to yellow–orange due to the formation of Mo(CO)$_3$(dppe)(THF). It became dark red upon bubbling SO$_2$ through the solution to form *fac*-Mo(CO)$_3$(dppe)(η^2-SO$_2$). The compound was obtained as dark red crystals (70 mg) from THF–toluene–pentane mixed solvent; yield 80%.

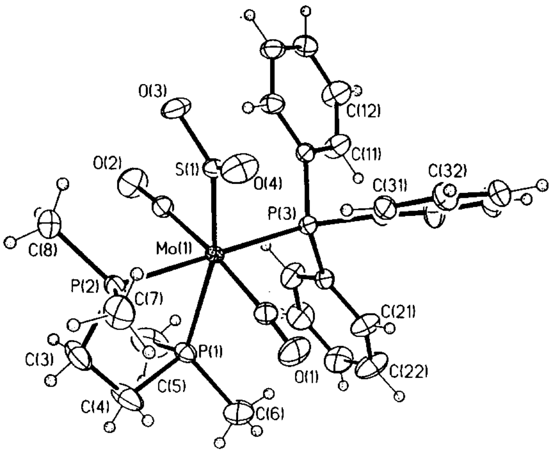

Fig. 1. Molecular structure of Mo(CO)$_2$(η^2-dmpe)(PPh$_3$)(SO$_2$) drawn with 40% thermal ellipsoids.

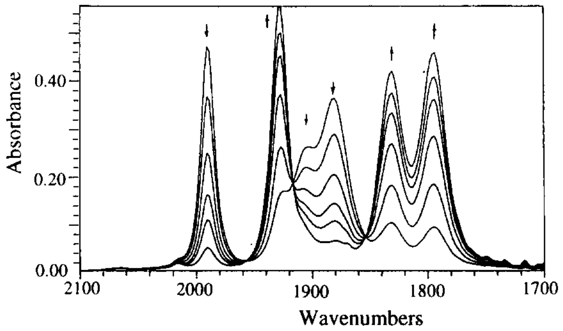

Fig. 2. IR spectra changes for reaction of *fac*-Mo(CO)$_3$(η^2-bipy)(η^2-SO$_2$) with P(OMe)$_3$ (Eq. (3)) in CH$_2$Cl$_2$.

2.3. Preparation of Mo(CO)$_2$(dmpe)(PPh$_3$)(SO$_2$)

350 mg of Mo(CO)$_2$(PPh)$_3$(η^2-SO$_2$)(NCMe) in 10 ml THF were mixed with 150 mg of dmpe (C$_2$H$_4$(PMe$_2$)$_2$) at 0 °C. The solution was stirred for 2 h. The solvent was reduced to 2–3 ml under reduced pressure. 10 ml of toluene were added through syringe and the solution was cooled to −20 °C. The product was obtained as an orange powder (150 mg, yield 53%). Deep red crystals were obtained from CH$_2$Cl$_2$–toluene–pentane mixed solvent. ^{1}H NMR (CD$_2$Cl$_2$): 0.83 (d, 6H); 1.75 (d, 6H); 1.2–1.8 (m, 4H); 7.4 (m, 9H); 7.6–7.7 (m, 6H). IR (CH$_2$Cl$_2$, ν(CO)): 1869 cm^{-1}. *Anal.* Calc. for C$_{25}$H$_{31}$MoO$_4$P$_3$S$_1$: C, 49.69; H, 4.94. Found: C, 49.37; H, 4.88%. The molecular structure is shown in Fig. 1.

The analogous complex Mo(CO)$_2$(dppe)(PPh$_3$)(SO$_2$) was made using the same method. It has ν(CO) at 1880 cm^{-1} in THF.

2.4. *Kinetics*

Kinetic experiments for SO_2 substitution of *fac*-$Mo(CO)_3(\eta^2\text{-L})(\eta^2\text{-}SO_2)$ were run under pseudo-first-order conditions, with the concentration of entering nucleophile in 10-fold excess or more. Kinetic data were obtained by following the appearance of the CO band of the product or the disappearance of that of the reactant (Fig. 2). The IR spectra were obtained on a Nicolet 5PC-FTIR spectrophotometer equipped with a P/N 20.500 variable temperature IR cell with 0.6 mm AgCl windows. Constant temperatures were obtained using a Neslab RTE-8 refrigeration circulating bath. In a typical experiment, 1.0 ml of *fac*-$Mo(CO)_3(dppe)(SO_2)$ CH_2Cl_2 solution (2×10^{-3} M) was mixed with 0.5 ml $P(n\text{-}Bu)_3$ (0.500 M) CH_2Cl_2 solution in a Schlenk tube which was kept at −78 °C. The mixed solution was then diluted with CH_2Cl_2 to 2 ml. The solution was transferred into the IR cell with syringe. After a few minutes for temperature equilibration, the IR spectrum changes were recorded. Plots of ln A_t (A_t is the absorbance of ν(CO) of the product) versus time were linear over two half-lives ($r^2>0.995$) for all the reactions. The slopes of these lines yield the observed rate constants. For the intramolecular ligand substitution of $Mo(CO)_2(\eta^1\text{-L})(PPh_3)_2(SO_2)$ (L = dppe or dmpe) to form $Mo(CO)_2(\eta^2\text{-L})(PPh_3)(SO_2)$ in THF solvent, rate constants were obtained by following the decrease of the CO stretching band of the reactant, using $\ln(A_t-A_\infty)=k_{obs}t+\text{constant}$. Plots of $\ln(A_t-A_\infty)$ versus time were linear over two half-lives ($r^2>0.995$). The reactants $Mo(CO)_2(\eta^1\text{-L})(PPh_3)_2(SO_2)$ were generated in situ by mixing the solution of $Mo(CO)_2(PPh_3)_2(\eta^2\text{-}SO_2)$-(NCMe) with those of the ligands at −78 °C. IR ν(CO) for $Mo(CO)_2(\eta^1\text{-dppe})(PPh_3)_2(SO_2)$ in THF: 1937, 1876 cm^{-1}. IR ν(CO) for $Mo(CO)_2(\eta^1\text{-dmpe})(PPh_3)_2$-$(SO_2)$ in THF: 1934, 1867 cm^{-1}.

2.5. *X-ray crystallographic structure determination*

Crystals were mounted on glass fibers. Preliminary photographic evidence revealed $2/m$ Laue symmetry. Systematic absences in the diffraction data uniquely fit the space group, $P2_1/c$. The data were empirically corrected for absorption. The structure was solved by direct methods. All non-hydrogen atoms were refined with anisotropic thermal parameters and hydrogen atoms were treated as idealized contributions. The phenyl rings were constrained to rigid, planar hexagons. At convergence the highest peak on the difference map was 0.62 e Å^{-3}. All computations used the SHELXTL program library (Version 4.2, G. Sheldrick, Siemens XRD, Madison, WI). For crystallographic data see Section 5.

$Mo(CO)_2(dmpe)(PPh_3)(\eta^1\text{-}SO_2)$ crystallizes as a distorted octahedral complex with *trans* CO groups. The SO_2 molecule is *trans* to one of the dmpe phosphorus atoms at an Mo–P distance 0.06 Å shorter than the other phosphorus atom of the chelating ligand, which is *trans* to PPh_3, and both are shorter by 0.03 Å than is typical of monophosphine–Mo distances in this and related complexes. The SO_2 ligand is planar (the sum of the bond angles about S is 359°) and rotated into the carbonyl plane to minimize interaction with the PPh_3 ligand. In the only precedent Mo–(η^1-SO_2) structure, that of $Mo(CO)_3(P\text{-}i\text{-}Pr_3)_2(SO_2)$ [9], the Mo–S distance is about 0.05 Å longer.

3. Results

Reaction of $Mo(CO)_2(PPh_3)_2(\eta^2\text{-}SO_2)(NCMe)$ with dppe or dmpe in THF at low temperature initially yields $Mo(CO)_2(\eta^1\text{-L})(PPh_3)_2(SO_2)$ (Eq. (4)).

$$Mo(CO)_2(PPh_3)_2(\eta^2\text{-}SO_2)(NCMe)+L \longrightarrow Mo(CO)_2(\eta^1\text{-L})(PPh_3)_2(SO_2)+NCMe \quad (4)$$

The η^1 complex undergoes facile intramolecular PPh_3 substitution to form $Mo(CO)_2(\eta^2\text{-L})(PPh_3)(SO_2)$ (Eq. (2)). The rate of PPh_3 substitution is first-order in the reactant complex. Rate constants and activation parameters are included in Table 1. Reactions of *fac*-$Mo(CO)_3(L)(\eta^2\text{-}SO_2)$ with various ligands yield SO_2 substituted compounds (Eq. (3)), which have their IR CO stretching frequencies (Table 2) consistent with those reported [11,12] for the complexes. The rates of reaction (Eq. (3)) increase with increasing concentrations of strong nucleophiles (Table 3), but the rates are independent of the concentration of weak nucleophiles (Fig. 3). First-order and second-order rate con-

Table 1
Rate constants and activation parameters for PPh_3 substitution of $Mo(CO)_2(\eta^1\text{-L})(PPh_3)_2(SO_2)$ (Eq. (2)) in THF

L	T (°C)	$10^4 k$ (s^{-1})	$\Delta H^{\ne}$ (kcal/mol)	$\Delta S^{\ne}$ (cal/mol K)
dmpe	4.5	3.06		
	15.0	7.26		
	26.0	16.3		
	26.0	15.6 [a]	12.3 ± 0.3	−30.3 ± 0.8
dppe	15.5	3.48		
	26.8	10.7		
	36.0	25.6	16.7 ± 0.2	−16.4 ± 0.6

[a] In the presence of added PPh_3 (0.14 M).

Table 2
IR CO stretching frequencies of the products *fac*-$Mo(CO)_3(\eta^2\text{-L})L'$ from SO_2 substitution reactions of *fac*-$Mo(CO)_3(\eta^2\text{-L})(\eta^2\text{-}SO_2)$ (Eq. (3)) with entering ligands in CH_2Cl_2

L	L′	IR ν(CO) (cm^{-1})
dppe	PMe_3	1937, 1841(b)
	PPh_3	1942, 1845(b)
	$P(OMe)_3$	1948, 1854(b)
	C_4H_8S	1931, 1839, 1820(sh)
bipy	$P(OMe)_3$	1927, 1831, 1795
	$P(n\text{-}Bu)_3$	1909, 1807, 1784

Table 3
Observed rate constants for SO_2 substitution reactions of *fac*-$Mo(CO)_3(\eta^2$-dppe$)(\eta^2$-$SO_2)$ (Eq. (3)) in CH_2Cl_2 at 22.5 °C

L	[L] (M)	$10^4 k_{obs}$ (s^{-1})
PMe_3	0.0439	5.00
	0.0878	5.56
	0.220	7.62
	0.439	10.1
P(n-Bu)$_3$	0.050	7.20
	0.100	9.76
	0.201	14.9
C_4H_8S	0.100	5.20
	0.566	6.75
	1.13	8.68

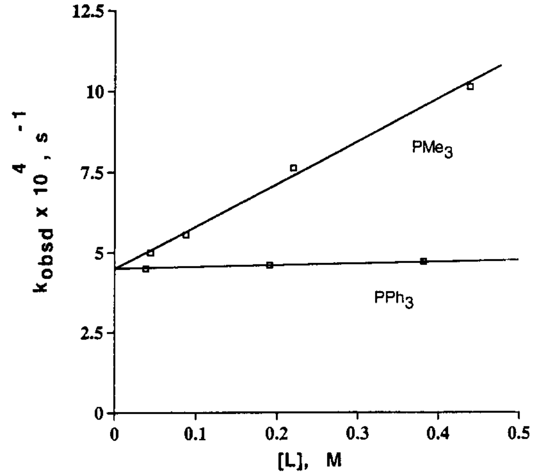

Fig. 3. Plot of observed rate constants vs. ligand concentrations for reaction of *fac*-$Mo(CO)_3(\eta^2$-dppe$)(\eta^2$-$SO_2)$ with PPh_3 and PMe_3 (Eq. (3)) in CH_2Cl_2.

stants as well as activation parameters are given in Tables 4 and 5, respectively.

4. Discussion

The reaction of *cis,trans*-$Mo(CO)_2(PPh_3)_2(\eta^2$-$SO_2)$-$(NCCH_3)$ [7] (see IV) with dppe ($Ph_2PC_2H_4PPh_2$) and with dmpe ($(Me)_2PC_2H_4P(Me)_2$) in THF solution at low temperatures initially affords $Mo(CO)_2(\eta^1$-L$)(PPh_3)_2$-(SO_2) (Eq. (4)), which is believed to have η^2-SO_2 [9].

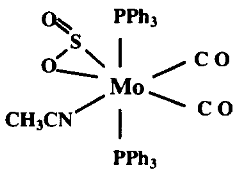

IV

The η^1-L complex formed then more slowly undergoes intramolecular PPh_3 substitution and chelating ring closure to form $Mo(CO)_2(\eta^2$-L$)(PPh_3)(SO_2)$ (Eq. (2)). The rate of PPh_3 substitution is first-order in concentration of the η^1-L complex; the rate constants and activation parameters are given in Table 1.

The low values of $\Delta H^{\neq}$ and the negative values of $\Delta S^{\neq}$ are indicative of nucleophilic attack on the metal and an associative mechanism. Further evidence to support the mechanism is that the rate of reaction is not affected by the presence of excess PPh_3, which would retard the rate of a dissociative process. Furthermore, it is expected that both base strength and steric factors would contribute to the relative ease of associative substitution reaction. The reaction of the dmpe complex has a lower $\Delta H^{\neq}$ value and a more negative $\Delta S^{\neq}$ value than does that of the dppe complex (Table 1), indicating more intensive interaction between the free end of the bidentate ligand and the metal atom in the reaction transition state for dmpe than for dppe. Substitution of PPh_3 in the *cis*-dicarbonyl complex $Mo(CO)_2(\eta^1$-dmpe$)$-$(PPh_3)_2(SO_2)$ yields exclusively the *trans*-dicarbonyl complex $Mo(CO)_2(\eta^2$-dmpe$)(PPh_3)(SO_2)$, as indicated by the X-ray structure of the product (Fig. 1). This would appear to be due to subtle electronic effects involving the SO_2 bonding [9] rather than steric preference. The SO_2 lies in the OC–M–CO plane, apparently to maximize π backbonding from the metal to the $2b_1$ orbital of SO_2. This orbital is located primarily on sulfur *orthogonal* to the plane of SO_2, and the observed SO_2 orientation would avoid competition with the CO ligands for backbonding [7a]. The isomer with *cis*-carbonyls could present a more unfavorable overall backbonding situation. Although the details of the molecular structure transformation are not clear, these results are also consistent with an associative reaction mechanism being in control of the substitution reaction.

This associative mechanism could result from the driving force to close the diphos chelate ring in going from η^1-L to the η^2-L product. Arguing against this is the earlier report [13] that CO substitution reactions of $Mo(CO)_5(\eta^1$-L$)$ (L = dppe or dmpe) to form $Mo(CO)_4(\eta^2$-L$)$ have near zero $\Delta S^{\neq}$ values (−1.7 cal/mol K for dmpe, 3.3 cal/mol K for dppe) and large $\Delta H^{\neq}$ values (28.7 kcal/mol for dppe, 28.2

Table 4
First-order rate constants for SO_2 substitution reactions of *fac*-$Mo(CO)_3(\eta^2$-dppe$)(\eta^2$-$SO_2)$ (Eq. (3)) in CH_2Cl_2 [a]

L	T (°C)	k_1 (s^{-1})
PMe_3	9.3	5.83×10^{-5}
	22.5	4.50×10^{-4}
	31.0	1.31×10^{-3}
PPh_3	22.5	4.60×10^{-4}
C_4H_8S	22.5	4.82×10^{-4}
P(n-Bu)$_3$	22.5	4.67×10^{-4}
P(OMe)$_3$	22.5	4.73×10^{-4}
P(OMe)$_3$	22.5	1.14×10^{-3} [b]

[a] Activation parameters calculated from k_1: $\Delta H_1^{\neq} = 24.2 \pm 2.0$ kcal/mol; $\Delta S_1^{\neq} = 7.8 \pm 3.8$ cal/mol K.

[b] First-order rate constant for the reaction of *fac*-$Mo(CO)_3(\eta^2$-bipy$)(\eta^2$-$SO_2)$.

Table 5
Second-order rate constants and activation parameters for SO_2 substitution reactions of *fac*-$Mo(CO)_3(\eta^2\text{-L})(\eta^2\text{-}SO_2)$ (Eq. (3)) with various ligands in CH_2Cl_2

Complexes	Entering ligands	T (°C)	k_2 ($s^{-1}M^{-1}$)	$\Delta H^{\neq}$ (kcal/mol)	$\Delta S^{\neq}$ (cal/mol K)
dppe	PMe_3	9.3	2.94×10^{-4}		
		22.5	1.30×10^{-3}		
		31.0	2.77×10^{-3}	17.3 ± 1.6	-13.5 ± 3.5
	$P(n\text{-}Bu)_3$	22.5	5.09×10^{-3}		
	C_4H_8S	22.5	3.42×10^{-4}		
bipy	$P(n\text{-}Bu)_3$	5.0	5.19×10^{-2}		
		12.5	7.97×10^{-2}		
		22.5	1.30×10^{-1}	8.0 ± 0.4	-35.5 ± 1.8
	$P(OMe)_3$	22.5	5.47×10^{-3}		

kcal/mol for dmpe), indicating primarily a dissociative process. If a nucleophilic attack on the metal made a major contribution to chelate ring closure then one would expect much more negative values of $\Delta S^{\neq}$ and lower values of $\Delta H^{\neq}$. The $\Delta H^{\neq}$ values are close to the Mo–CO bond dissociation energy [14] (~30 kcal/mol) suggesting that the chelating effect does not play a significant role in these reactions.

In contrast the corresponding molybdenum compounds used in our studies do have negative $\Delta S^{\neq}$ values and low $\Delta H^{\neq}$ values (Table 1), consistent with an associative nucleophilic displacement process. Considering the difference between the two compounds $Mo(CO)_5(\eta^1\text{-L})$ and $Mo(CO)_2(\eta^1\text{-L})(PPh_3)_2(SO_2)$, it is seen that three of the COs of the pentacarbonyl are replaced by two PPh_3 and one SO_2. Since CO is a strong π-acid and since PPh_3 and SO_2 are stronger bases than CO, it follows that the electron density on Mo would be much higher in the present compound than in the pentacarbonyl. Also it is clear that Mo in the present compound would be much more sterically hindered than in the pentacarbonyl.

Both the higher electron density on Mo and its steric crowding would tend to retard nucleophilic attack on Mo, yet the kinetic data (Table 1) suggest otherwise. Since the results of the pentacarbonyl study [13] suggest chelate ring closure is not responsible for an associative pathway, one is prompted to designate the role of SO_2 as the ligand allowing for an $\eta^2\rightarrow\eta^1$-pyramidal$\rightarrow\eta^1$-planar reaction mechanism via an 18-e intermediate or transition state (Scheme 1).

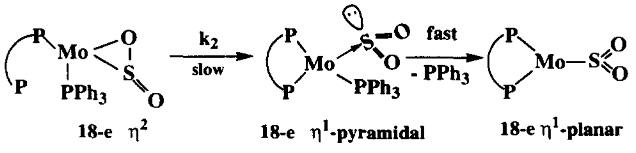

(2 COs and 1 PPh_3 not shown)

Scheme 1.

Interestingly, the reactions of *fac*-$Mo(CO)_3(\eta^2\text{-L})(\eta^2\text{-}SO_2)$ (L = dppe, bipy) with entering ligands yield SO_2 substituted products. The rates for the reactions of the dppe complex with $P(n\text{-}Bu)_3$ and PMe_3 increase with increasing ligand concentrations (Table 3). Plots of observed rate constants versus ligand concentrations yield straight lines with non-zero intercepts (Fig. 3). The results indicate that the reaction proceeds by both associative and dissociative mechanisms for the same entering ligand. This is further supported by the fact that the intercepts of the plots of observed rate constants versus ligand concentrations are all the same at the same temperature for different ligands, indicating that the dissociative rate constants (k_1) are not dependant on the properties of the entering ligands. The associative rate constants (k_2) for the reaction vary with the different ligands as nucelophiles. It is noted that PMe_3 reacts with the complex more slowly than does $P(n\text{-}Bu)_3$, which is opposite to what is usually observed in associative organometallic reactions [4]. Although PMe_3 has σ-donicity (the ability of a ligand to donate σ-electrons to a transition metal [16]) ($\chi=8.65$) a little weaker than that of $P(n\text{-}Bu)_3$ ($\chi=5.25$, χ is the IR shift of the a_1 CO stretching band of $Ni(CO)_3L$ in wavenumbers relative to that of $Ni(CO)_3P(t\text{-}Bu)_3$ [15]), its cone angle ($\theta=118°$) is considerably smaller than that of $P(n\text{-}Bu)_3$ ($\theta=132°$) [15a]. That the rate of reaction of the dppe complex is faster with $P(n\text{-}Bu)_3$ than with PMe_3 indicates that the dppe complex is not sensitive to the steric effects of the ligands. The complex may be sterically so crowded that the metal–phosphine ligand bond in reaction transition state is not strongly formed. Thus, the relatively long Mo–P bond distance would reduce the importance of entering ligand steric effects. This argument is consistent with the relatively high activation enthalpy (Table 5) obtained for the reaction. The reaction (Eq. (3)) with phosphine proceeded more rapidly in THF than in CH_2Cl_2, but the kinetics are complicated probably due to the involvement of the THF solvent. It is observed that the complex is in equilibrium with $Mo(CO)_3(dppe)(THF)$ in THF solvent in the absence of other ligands. The increase in rate for the reaction (Eq. (3)) in THF solvent may be caused by nucleophilic attack of THF on the metal to replace SO_2 followed by a THF substitution reaction with the entering ligand. Kinetic studies show that tetrahydrothiophene can replace SO_2 in *fac*-$Mo(CO)_3(\eta^2\text{-dppe})(\eta^2\text{-}SO_2)$ by both dissociative and associative mechanisms in CH_2Cl_2. One referee pointed out that the rates of the reactions increase in the order $C_4H_8S < PMe_3 < P(n\text{-}Bu)_3$ which is also consistent with a reaction mechanism in which

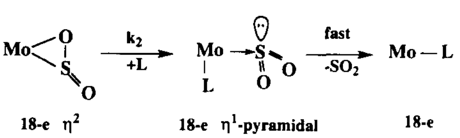

(3 COs and dppe are not shown)

Scheme 2.

there is a preequilibrium between the complex and its ligand addition product, followed by rate-determining loss of SO_2, since SO_2 dissociation would be accelerated by large ligands.

It was reported that $Mo(CO)_4(dppe)$ reacted with phosphine or phosphite ligands by a dissociative mechanism to yield CO substituted products [17]. Replacement of CO by the SO_2 ligand enhanced the reactivity of the metal complex for both dissociative and associative ligand substitution. The increase in the rate of ligand dissociation for the SO_2 complex is due to the low SO_2 dissociation energy ($\Delta H^{\neq} = 24$ kcal/mol) compared with that of CO ($\Delta H^{\neq} = 38$ kcal/mol for $Mo(CO)_4(dppe)$) [17]. It is believed that the facile associative path for SO_2 substitution is due to the ability of SO_2 to transform η^2-side-on to η^1-pyramidal coordination in the reaction transition state, thus allowing the complex to maintain a stable 18-e count (Scheme 2).

Nucleophile induced SO_2 coordination transformation from η^1-planar to η^1-pyramidal was reported for *trans*-$Ir(SO_2)(Cl)(PR_3)_2$ [18]. The iridium complex reacts with CO at low temperatures to form the five-coordinated CO adduct, in which SO_2 has an η^1-pyramidal configuration. This adduct loses its SO_2 ligand at higher temperatures (Eq. (5)).

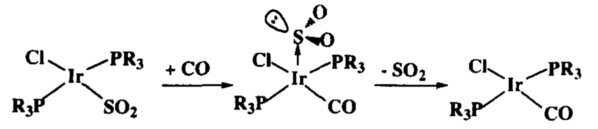

(5)

Since the reaction of $Mo(CO)_3(bipy)(\eta^2\text{-}SO_2)$ with PMe_3 is too fast to follow using convenient methods, its slower reaction with $P(n\text{-}Bu)_3$ was studied instead. The results show the reaction proceeds mainly by an associative mechanism with the phosphine ligand. The dissociative rate constant was better defined in its reaction with $P(OMe)_3$. The rate for SO_2 dissociation is about two times faster for the bipy complex than for the dppe complex (Table 4). This observation is consistent with that observed in CO substitution reactions of bipy metal complexes, where bipy has *cis*-labilizing effects on ligand dissociation [12,19,20]. The rate for the associative reaction pathway is about 25 times faster for the bipy complex than for the dppe complex at 22.5 °C (Table 5). This significant increase in the second-order rate constants for the bipy complex may be due to the lower steric hindrance of the bipy ligand compared with the dppe ligand. This is consistent with the bipy complex being very sensitive to the size of the entering ligands (rates $PMe_3 \gg P(n\text{-}Bu)_3$), whereas the dppe complex is rather insensitive to the entering ligand size ($PMe_3 < P(n\text{-}Bu)_3$).

5. Supplementary material

Tables of crystallographic data, bond distances and angles, anisotropic thermal parameters and hydrogen-atom coordinates for $Mo(CO)_2(dmpe)(PPh_3)(SO_2)$ are available from author A.L.R. on request.

Acknowledgements

J.K.S. thanks Northwestern University for support of this research, and thanks Professor F. Basolo for valuable discussions. G.J.K. thanks the US Department of Energy, Division of Chemical Sciences, Office of Basic Energy Sciences, for funding. A.L.R. thanks the National Science Foundation for support of this research.

References

[1] E.M. Thorsteinson and F. Basolo, *J. Am. Chem. Soc., 88* (1966) 3929.
[2] H.G. Schuster-Wolden and F. Basolo, *J. Am. Chem. Soc., 88* (1966) 1657.
[3] F. Zingales, A. Chiesa and F. Basolo, *J. Am. Chem. Soc., 88* (1966) 2707.
[4] (a) J.M. O'Connor and C.P. Casey, *Chem. Rev., 87* (1987) 307; (b) J.P. Collman, L.S. Hegedus, J.R. Norton and R.G. Finke, *Principles and Applications of Organotransition Metal Chemistry*, University Science Books, Mill Valley, CA, 1987.
[5] D.J. Hodgson and J.A. Ibers, *Inorg. Chem., 8* (1969) 1282.
[6] D.F. Shriver, P.W. Atkins and C.H. Langford, *Inorganic Chemistry*, Oxford University Press, Oxford, 2nd edn., 1994, p. 208.
[7] (a) R.R. Ryan, G.J. Kubas, D.C. Moody and P.G. Eller, *Struct. Bonding (Berlin), 46* (1981) 47; (b) W.A. Schenk, *Angew. Chem., 26* (1987) 981.
[8] J.K. Shen, F. Basolo and G.J. Kubas, *J. Organomet. Chem., 488* (1995) C1.
[9] G.J. Kubas, G.D. Jarvinen and R.R. Ryan, *J. Am. Chem. Soc., 105* (1983) 1883.
[10] F. Zingales and F. Canziani, *Gazz. Chim. Ital., 92* (1962) 343.
[11] (a) M.H.B. Stiddard, *J. Chem. Soc.*, (1963) 756; (b) G.R. Dobson and L.A.H. Smith, *Inorg. Chem., 9* (1970) 1001.
[12] J.R. Graham and R.J. Angelici, *J. Am. Chem. Soc., 87* (1965) 5590.
[13] J.A. Connor and G.J. Hudson, *J. Organomet. Chem., 73* (1974) 351.
[14] (a) R.J. Angelici and J.R. Graham, *J. Am. Chem. Soc., 88* (1966) 3658; (b) *Inorg. Chem., 6* (1967) 2082.
[15] (a) C.A. Tolman, *Chem. Rev., 77* (1977) 313; (b) T. Bartik, T. Himmler, H.G. Schulte and K. Seevogel, *J. Organomet. Chem., 272* (1984) 29.
[16] M.M. Rahman, H.Y. Liu, K. Eriks, A. Prock and W.P. Giering, *Organometallics, 8* (1989) 1.
[17] G.C. Faber and G.R. Dobson, *Inorg. Chim. Acta, 2* (1968) 479.
[18] W.A. Schenk and J. Leißner, *J. Organomet. Chem., 311* (1986) C27.
[19] R.J. Angelici and J.R. Graham, *J. Am. Chem. Soc., 87* (1965) 5586.
[20] (a) J.D. Atwood and T.L. Brown, *J. Am. Chem. Soc., 97* (1975) 3380; (b) D.L. Lichtenberger and T.L. Brown, *J. Am. Chem. Soc., 100* (1978) 366; (c) T.L. Brown and J.D. Atwood, *J. Am. Chem. Soc., 98* (1976) 3160.